

Explosive production of Higgs particles and implications for heavy dark matter

Seishi Enomoto,^{1,2,3} Nagisa Hiroshima,^{2,4} Kohta Murase,^{5,6,7} and Masato Yamanaka^{2,8,9}

¹*School of Physics, Sun Yat-sen University, Guangzhou 510275, China*

²*Department of Physics, Faculty of Engineering Science,
Yokohama National University, Yokohama 240-8501, Japan*

³*Department of Science and Engineering, Faculty of Electrical Engineering,
Kyushu Sangyo University, Fukuoka 813-8503, Japan*

⁴*RIKEN Center for Interdisciplinary Theoretical and Mathematical Sciences(iTHEMS), RIKEN, Wako 351-0198, Japan*

⁵*Department of Physics, The Pennsylvania State University, University Park, Pennsylvania 16802, USA*

⁶*Department of Astronomy and Astrophysics, The Pennsylvania State University, University Park, Pennsylvania 16802, USA*

⁷*Center for Multimessenger Astrophysics, The Pennsylvania State University, University Park, Pennsylvania 16802, USA*

⁸*Department of Advanced Sciences, Faculty of Science and Engineering, Hosei University, Tokyo 184-8584, Japan*

⁹*Department of Literature, Faculty of Literature,
Shikoku Gakuin University, Kagawa 765-8505, Japan*

(Dated: April 25, 2025)

It is widely believed that the parameter space for Higgs-portal dark matter that achieves the relic abundance through thermal freeze-out has already been tightly constrained, typically at masses on the order of $\mathcal{O}(10 - 100)$ GeV. We point out the possibility that the multiple Higgs production due to its self-interaction dramatically changes this picture. We show that the multiplicity can be as large as $\mathcal{O}(200)$ for the parameters of the Standard Model Higgs, independently of the kinematics of the particle production process. Consequently, heavy Higgs-portal dark matter of $m_\chi \gtrsim \mathcal{O}(1)$ TeV can achieve the required relic abundance in the same mechanism with that for canonical weakly interacting massive particle models.

Introduction—The nature of dark matter (DM) is a long-standing puzzle in particle physics and cosmology (e.g., [1, 2]). The most appealing framework to generate DM is the thermal freeze-out mechanism, which links the DM relic density and the properties of particle DM independently of the initial conditions in the early Universe. Within this framework, carrying out a detailed computation of the relic density comes to understand the DM nature.

The discovery of the Higgs boson has opened new doors for exploring fundamental physics beyond the standard model (SM), such as the nature of DM. There are still mysteries to be unraveled in the Higgs sector, such as the origin of the electroweak symmetry breaking and the number of Higgs fields. Unified pictures for describing the nature of Higgs fields and DM have been proposed and argued in a large amount of literature [3–19]. An attractive scenario among them is the so-called Higgs portal DM scenario, in which the SM Higgs field acts as a bridge between the fundamental theory behind DM and our world. The observed DM abundance in these scenarios is achieved through the resonant annihilation of DM to the SM Higgs boson, and then the DM mass is required to be $\simeq m_H/2$, where $m_H \simeq 125$ GeV is the Higgs boson mass [20].

The possibility of the *Higgspllosion*, which is an exponential growth of the decay rate of highly-excited Higgs boson into multiple Higgs bosons, is pointed out in Refs. [21–25]: This cannot be tested with the current facilities due to the kinematical limitation. However, it would be possible with future collider experiments [26–28]. Studies of factorial growth of the multiparticle pro-

duction amplitude have a long history [29–32]. The production cross sections show a characteristic exponential form, $\sigma_n \propto \exp[nF(g, n)]$, where $F(g, n)$ is a function of the coupling g and the multiplicity n . Although the naive consideration about the Higgspllosion may result in the continuous growth of multiparticle production as the energy scale gets higher, the perturbative approach breaks down when the theory becomes strongly coupled and more than $\mathcal{O}(100)$ Higgs bosons are produced [21, 22, 26]. At such high energies, the dressed propagator plays an important role in preserving the unitarity and regulating the multiparticle production, which is called the Higgsperion effect. Details about the competition between the Higgspllosion and Higgsperion are not yet fully investigated.

This Letter focuses on the explosive Higgs production in DM annihilation, incorporating the effects from the Higgsperion, then addresses its phenomenological consequences, such as the DM freeze-out in the early universe [33]. The balance between the Higgspllosion and the Higgsperion is nontrivial: the annihilation of heavy DM of $\gtrsim \mathcal{O}(1)$ TeV generates an energy clump, which transits into n -Higgs bosons ($n \gg 1$) before emitting a large number of final-state particles. However, as we show below, the Higgs multiplicity in this transition is uniquely determined by the value of the Higgs self-coupling λ by taking the thermal average of the DM annihilation cross section. Such a mechanism enhances the effective reaction rate between the DM and the SM thermal bath, allowing heavier DM compared with those in simple Higgs portal scenarios.

Setup and Formulation—We minimally extend the SM

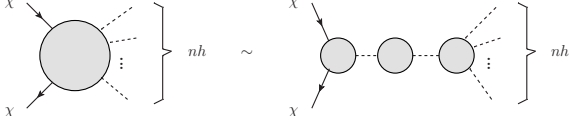


FIG. 1. Schematic picture of our approximation in the calculation of the scattering amplitude for $\chi\chi \rightarrow nh$.

with a fermionic DM χ which couples to the SM Higgs field ϕ to demonstrate the Higgspllosion effect on DM relic density. The formulation here is applicable to DM scenarios with other scalar fields. We introduce the Lagrangian as

$$\mathcal{L} = \frac{1}{2}(\partial\phi)^2 - \frac{1}{4}\lambda(\phi^2 - v^2)^2 + \bar{\chi}(i\cancel{\partial} - m_\chi)\chi - (y_\chi\phi\bar{\chi}_R\chi_L + \text{h.c.}), \quad (1)$$

where v is the vacuum expectation value of the Higgs field. In general, the Yukawa coupling y_χ is a complex while the DM mass m_χ is chosen to be real by rotating the phase of the left- and right-handed fermion fields independently. Redefining the left-handed DM field as $e^{i\arg M_\chi}\chi_L \rightarrow \chi_L$, the DM mass is

$$M_\chi \equiv m_\chi + y_\chi v = |M_\chi|e^{i\arg M_\chi}. \quad (2)$$

Then, the Lagrangian (1) is represented as

$$\mathcal{L} = \frac{1}{2}(\partial h)^2 - \frac{1}{2}m_h^2 h^2 - \lambda v h^3 - \frac{1}{4}\lambda h^4 + \bar{\chi}(i\cancel{\partial} - |M_\chi|)\chi - h\bar{\chi}(\tilde{y}_\chi P_L + \tilde{y}_\chi^* P_R)\chi, \quad (3)$$

where we denote $h = \phi - v$, $m_h^2 = 2\lambda v^2$, $\tilde{y}_\chi = y_\chi e^{-i\arg M_\chi}$, and $P_{L(R)}$ is the chirality projection operator. In the nonrelativistic regime, for real \tilde{y}_χ , the annihilation is p -wave dominant and suppressed due to low velocity. On the other hand, the s -wave dominant contribution is achieved for complex cases. A nonzero value of m_χ is required for $\text{Im}\tilde{y}_\chi \neq 0$ because $\tilde{y}_\chi = y_\chi e^{-i\arg y_\chi} = |y_\chi|$ holds for $M_\chi = 0$.

DM annihilation with the Higgspllosion effect—We consider DM that is much heavier than the SM Higgs, $|M_\chi| \sim nm_h$ with $n \sim \mathcal{O}(100)$. We apply the formulation of the Higgspllosion phenomenon to the thermally averaged cross section of DM annihilation, $\chi\chi \rightarrow nh$. The intermediate state in the DM annihilation process is highly excited, and its decay rate exponentially grows with the final multiplicity.

We decompose the scattering amplitude for the process $\chi\chi \rightarrow nh$ into three components: (i) an effective vertex on DM annihilation $\chi\chi \rightarrow h^*$, (ii) a dressed propagator on $h^* \rightarrow h^*$, and (iii) an effective vertex on $h^* \rightarrow nh$ (see FIG. 1). This prescription is applicable whenever the s -channel type diagram dominates over those from t - and/or u -channel type processes, $\chi\chi \rightarrow h^*h^* \rightarrow n'h + (n - n')h$, where n' is an integer smaller than n . We will show later that the above situation is generally realized.

With this prescription, the squared amplitude is obtained as

$$\sum_{\text{spins}} |\mathcal{M}(\chi\chi \rightarrow nh)|^2 \sim \sum_{\text{spins}} \left| \mathcal{M}(\chi\chi \rightarrow h) \frac{1}{s - M_h(s)^2 - iM_h(s)\Gamma_h(s)} \mathcal{M}(h \rightarrow nh) \right|^2 \quad (4)$$

$$\sim 2|\tilde{y}_\chi|^2 (s - 4|M_\chi|^2 \cos^2 \theta_{\tilde{y}}) \frac{1}{s^2 + m_h^2 \Gamma_h(s)^2} |\mathcal{M}(h \rightarrow nh)|^2, \quad (5)$$

where we denote $\theta_{\tilde{y}} \equiv \arg \tilde{y}_\chi$, $M_h(s)$ as the effective mass of h including the self-energy correction, and $\Gamma_h(s)$ as the total width of the virtual h . We approximate the effective vertex on $\chi\chi \rightarrow h^*$ by the elementary one in the Lagrangian (3), and apply $M_h(s) \sim m_h \ll \sqrt{s}$ in this calculation.

The annihilation cross section associated with all n contributions of the Higgspllosion process $\chi\chi \rightarrow nh$ is evaluated using Eq. (5) as

$$\sigma = \sum_n \sigma_{\chi\chi \rightarrow nh} = \frac{1}{\sqrt{s(s - 4|M_\chi|^2)}} \cdot \frac{|\tilde{y}_\chi|^2}{4} \times \left(1 - \frac{4|M_\chi|^2 \cos^2 \theta_{\tilde{y}}}{s} \right) W(s) \quad (6)$$

Here we introduced a “window” function $W(s)$

$$W(s) = \frac{2sm_h^2 \mathcal{R}(s)}{s^2 + m_h^4 \mathcal{R}(s)^2}, \quad 0 \leq W(s) \leq 1, \quad (7)$$

with the dimensionless reaction rate $\mathcal{R}(s) = \Gamma_h(s)/m_h$, which is an exponentially increasing function at $\sqrt{s} \gtrsim 100m_h$. See *Supplemental Material* for the details. The window function $W(s)$ consists of the Higgs dressed propagator and the Higgsploding vertex on the process $h^* \rightarrow nh$.

As mentioned above, the reaction rate $\mathcal{R}(s)$ for the $h^* \rightarrow nh$ process exponentially grows as $n \sim \sqrt{s}/m_h$ increases. Simultaneously, the dressed propagator regulates the exponential growth of $\mathcal{R}(s)$ in the denomina-

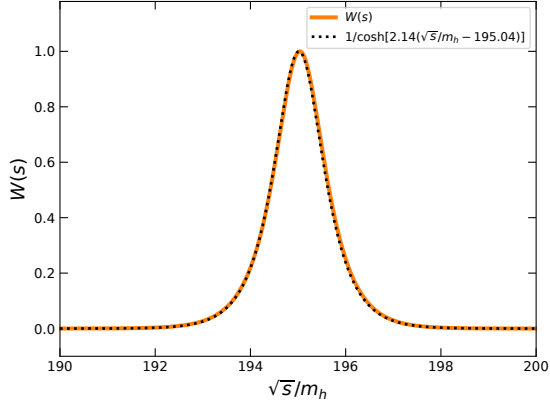


FIG. 2. The shape of the window function. The peak position is $\sqrt{s_{\text{peak}}}/m_h = 195.04$. The window function can be well-fitted as $W(s) \sim 1/\cosh[2.14(\sqrt{s} - \sqrt{s_{\text{peak}}})/m_h]$.

tor of (14) at large s (Higbspersion effect). The window function $W(s)$ characterizes the balance between the Higbsplosion and the Higbspersion: a smaller or larger $\mathcal{R}(s)$ provides a suppression factor in (6), while the window opens ($W(s) \sim 1$) at a certain point $s = s_{\text{peak}}$ satisfying the peak condition $s_{\text{peak}} = m_h^2 \mathcal{R}(s_{\text{peak}})$. Both the peak position and the shape of the window function $W(s)$ depend only on the Higgs self-coupling λ . Using $\lambda = 0.129$,

the peak appears at $\sqrt{s_{\text{peak}}} \simeq 195m_h$ with a finite width of $\Delta\sqrt{s} \simeq \pm 1m_h$ (see FIG. 2). This means that the process $\chi\chi \rightarrow 195h$ has the leading contribution among the annihilation channels to various n .

The structure of the window in the s -channel type process explains the reason this process dominates over the t - or u -channel types. The contribution from t - or u -channel type processes is regarded as the double Higbsplosion process of $\chi + \chi \rightarrow h^* + h^* \rightarrow n'h + (n - n')h$. If the multiplicity of the two Higgs in the intermediate process is similar ($n' \sim n/2$), then the spectrum cannot fit the window. On the other hand, if one of the intermediate-state Higgs takes most of the multiplicity ($n' \ll n$), then the process is that of a Higbsplosion with an additional external Higgs; hence the additional suppression factor $(\tilde{y}_\chi/\sqrt{4\pi})^{n'}$ compared to the s -type process is expected [34].

Here we emphasize the important role of the phase of the coupling \tilde{y}_χ . As seen in Eq. (6), a pure imaginary \tilde{y}_χ ($\theta_{\tilde{y}} = \pm\pi/2$) leads to the s -wave annihilation, while a real \tilde{y}_χ ($\theta_{\tilde{y}} = 0$) leads to the p -wave feature because the cross section is proportional to the momentum of χ , $\sqrt{s - 4|M_\chi|^2} \sim |\vec{p}_\chi|$. The cross section of the DM pair-annihilation into two Higgs bosons serves as a good reference. It is evaluated as

$$\sigma(\chi\chi \rightarrow hh) \sim \frac{1}{\sqrt{s(s - 4|M_\chi|^2)}} \cdot \frac{|\tilde{y}_\chi|^4}{16\pi} \left[\sin^2 2\theta_{\tilde{y}} + \frac{1}{3}(4\cos^2 \theta_{\tilde{y}} - 1)^2 \left(1 - \frac{4|M_\chi|^2}{s} \right) + \dots \right] \quad (8)$$

in the limit of $\sqrt{s} \gg m_h$. The first and second terms inside the brackets correspond to the s - and p -wave contributions, respectively. As is shown in Eqs. (8) and (6), at low-momentum regimes, the pure imaginary \tilde{y}_χ damps the 2-to-2 annihilation, and while it maximizes the 2-to- n annihilation processes.

Boltzmann equation and numerical results—The cross-section incorporating the Higbsplosion is now applied to the evaluation of thermal relic abundance. The Boltzmann equation for the DM number density is

$$\dot{n}_\chi + 3Hn_\chi = -\langle\sigma v\rangle (n_\chi^2 - (n_\chi^{\text{eq}})^2), \quad (9)$$

where H is the Hubble parameter. n_χ and n_χ^{eq} are the actual and equilibrium number density of DM, respectively. Here, we assume the kinetic equilibrium between DM and background SM fields. The thermally-averaged cross section is derived using Eq. (6) as

$$\langle\sigma v\rangle = \frac{1}{(n_\chi^{\text{eq}})^2} \cdot \frac{|\tilde{y}_\chi|^2}{32\pi^4} T^4 \int_{4|M_\chi|^2}^{\infty} \frac{ds}{s} \rho(\sqrt{s}/T) W(s) \quad (10)$$

where T is the temperature and

$$\rho(\sqrt{s}/T) = \frac{\sqrt{s - 4|M_\chi|^2} (s - 4|M_\chi|^2 \cos^2 \theta_{\tilde{y}})}{T^3} K_1(\sqrt{s}/T) \quad (11)$$

describes the spectrum of the scattering. $K_n(x)$ is the n -th modified Bessel function.

FIG. 3 shows the numerical results with $\lambda = 0.129$, $m_h = 50$ GeV and $\tilde{y}_\chi = 1.30i$. Each line corresponds to a different DM mass case. The reason for the small Higgs mass $m_h = 50$ GeV < 125 GeV is that the freeze-out era is expected in electroweak symmetry breaking. The freeze-out temperature of the DM annihilation can be estimated as $T_f \sim |M_\chi|/25 \sim \frac{1}{2}nm_h/25 \sim 200$ GeV $\times (m_h/50\text{GeV})$ for $n \sim 200$. This temperature must be lower than the electroweak symmetry breaking scale, since otherwise the Higgs particle is massless.

In the upper panel of FIG. 3, the ratio of the reaction rate $n_\chi\langle\sigma v\rangle$ to the Hubble parameter H is shown. The annihilation process freezes out when the ratio reaches the order of unity. As shown in the figure, the maximum reaction rate is achieved at $2|M_\chi| \sim 194m_h$, which is

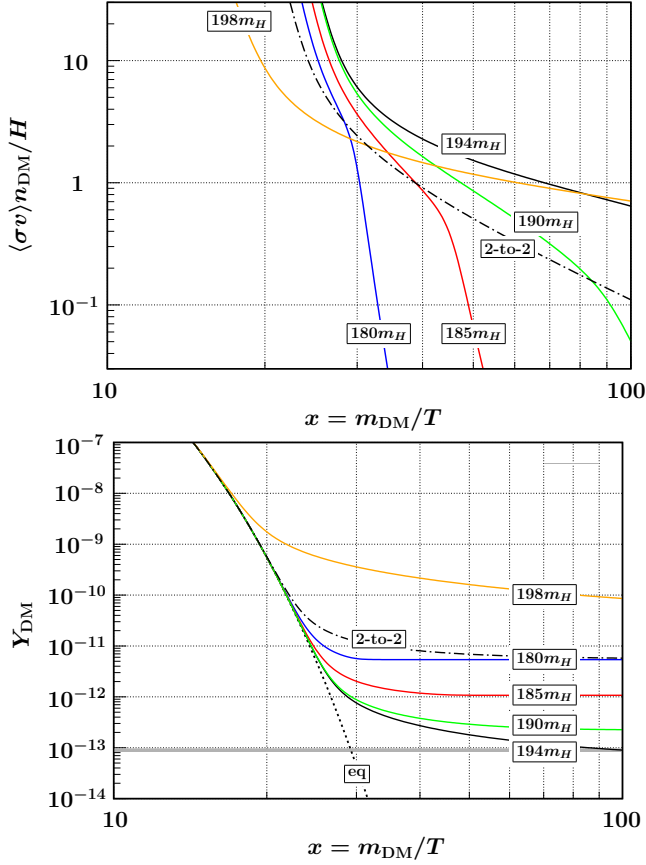


FIG. 3. Evolution of the ratio of reaction rates to the Hubble parameter (upper panel) and the yield of DM (bottom panel) for each DM mass. Parameters are set as $\lambda = 0.129$, $m_h = 50$ GeV, and $\tilde{y}_\chi = 1.30i$. The results by the 2-to-2 scattering process ($\chi\chi \rightarrow 2h$) are evaluated based on (8) with $2|M_\chi| = 194m_h = 2 \times 4.85$ TeV.

slightly smaller than the window peak $\sqrt{s_{\text{peak}}} = 195m_h$. For heavier DM cases of $2|M_\chi| \gtrsim 194m_h$, the scattering spectrum in (17) is always out of the window since $s > \sqrt{s_{\text{peak}}}$. At this regime, its cross section damps. On the other hand, for cases of $2|M_\chi| \lesssim 194m_h$, although the window function still opens, the dominant contribution in the cross-section spectrum (11) does not match the window range due to the Boltzmann suppression in $K_1(\sqrt{s}/T)$. Consequently, the DM with $2|M_\chi| \sim 194m_h$ can be in the chemical equilibrium for the longest time and reduce the DM yield sufficiently.

In the lower panel, we show the DM yield $Y_\chi = n_\chi/s$, where $s = \frac{2\pi^2}{45}g_{*S}T^3$ is the entropy density. Here g_{*S} denotes the total number of relativistic degrees of freedom. The current observation requires $Y_{\chi,\text{now}} = 8.99 \times 10^{-14}$ ($4.85 \text{ TeV}/|M_\chi|$) [35]. Our calculation finds $Y_\chi(x=100) = 9.08 \times 10^{-14}$ for $2|M_\chi| = 194m_h = 2 \times 4.8 \text{ TeV}$, and hence this representative parameter set successfully accounts for the relic abundance.

We here comment on the smaller reaction rates than that of the 2-to-2 annihilation channel in FIG. 3, the re-

sults for $2|M_\chi| = 180m_h$ and $185m_h$. This unexpected result originates from applying the dimensionless reaction rate $\mathcal{R}(s)$ to the 2-to-2 process. The $\mathcal{R}(s)$ is computed in the non-relativistic limit of the final state particles. For low-multiplicity production processes, this limit is no longer applicable. In our computation of the total cross section, however, all channels of n -body final states are summed over by applying the $\mathcal{R}(s)$ regardless of the limited applicability. The contributions from low-multiplicity processes are small compared to those of high-multiplicities. (See *Supplemental material* for details.) It is rational and acceptable for the purpose of highlighting the feature of the Higgspllosion. The complete Higgsploding cross section, as a practical matter, is always larger than the case of the 2-to-2 process.

Discussion—This work highlights the impact of the Higgspllosion phenomenon on the relic abundance of Higgs-portal DM, taking a simplified setup of a minimally extended model. It can drastically change the DM abundance in Higgs-portal DM models, but further investigations are needed to obtain a conclusive picture. There are several issues to be investigated. For example, quantum statistical effects for the high-multiplicity state would change the evolution of the relic density by distorting the shape of the window function. Further enhancement of the thermally-averaged cross section through the stimulated emission would be expected if the Bose-Einstein statistics is applied. A careful formulation of the intermediate dressed state, where the correlation function is regulated by thermal damping and Debye mass, which is beyond the scope of this work.

The signatures in the current Universe should be carefully searched for. In the model we discussed here, the DM annihilation to high-multiplicity final states cannot be expected in the current Universe. This is because $m_h = 125$ GeV has already been achieved, and the kinematically allowed Higgs-multiplicity is $2|M_\chi|/m_h^{T=0} \sim 77$, which is outside the window function. Therefore, the energetic 2- or 3-body Higgs final state is the leading DM annihilation channel. From Eq. (8), the maximal annihilation cross section is $\sigma v(\chi\chi \rightarrow 2h) \simeq |\tilde{y}_\chi|^4/32\pi M_\chi^2$, and is numerically $1.41 \times 10^{-26} \text{ cm}^3\text{s}^{-1}$ for $|\tilde{y}_\chi| = 1.30$ and $M_\chi = 4.85 \text{ TeV}$. This is slightly smaller than the current bounds from indirect detection experiments $\sigma v|_{\text{obs.}} \lesssim 5 \times 10^{-25} \text{ cm}^3\text{s}^{-1}$ for $M_\chi = 4.85 \text{ TeV}$ [36]. Future observation (e.g. [37, 38]) will be able to probe the signature. Null results from direct searches for DM ruled out some of the parameters that characterize DM. An idea to evade direct detection bounds is to make the DM a Majorana state [39]. It is realized by considering a minimal extension with a singlet Majorana fermion Ψ and two kinds of $SU(2)_L$ fermions: $f_L = (f^-, f^0)^T$ and $f_R = (f'^-, f'^0)^T$ of which the Lagrangian includes terms $-\frac{1}{2}\bar{\Psi}(m_\psi P_L + m_\psi^* P_R)\Psi - m_D \bar{f}f - (\bar{\Psi}(y_L P_L + y_R P_R)H \cdot f + \text{h.c.})$. We take pos-

itive m_D and $y_{L,R}$ without losing generality, while m_ψ is a complex. In the mass eigenbasis, the interactions of the lightest state χ_1 , which is DM, with the SM Higgs and the Z boson are parametrized as $h\bar{\chi}_1(c_h + ic_5\gamma^5)\chi_1$ and $c_Z Z_\mu \bar{\chi}_1 \gamma^\mu \gamma^5 \chi_1$. The coefficients c_h and c_Z are constrained from spin-independent and spin-dependent direct detection experiments (e.g. [39]). For typical scales expected from the DM relic abundance in our setup, e.g., $m_\psi = i \times 5 \text{ TeV}$ and $m_L = m_{\bar{L}} = 1 \text{ TeV}$, then $|c_h| \simeq \frac{y_L y_R v}{m_D} \frac{\text{Re } m_\psi}{|m_\psi|} = 0$ and $|c_Z| \simeq \frac{g_2}{4 \cos \theta_w} \frac{|y_L^2 - y_R^2| v^2}{2m_D^2} = 0$ in the mostly-singlet limit, where $|m_D| \gg |m_\psi|$, $|m_L|$, $|m_{\bar{L}}|$ and $y_L = y_R$. The remaining coupling, c_5 , is difficult to constrain with current facilities [40].

Our results are applicable to other scenarios, where the DM annihilates into neutral scalars. The important ingredient is the window function $W(s)$; the self-coupling constant of neutral scalars shapes it, and its width and peak position govern the final state multiplicity. A highlighted difference between the DM scenarios with general scalars and SM Higgs is the final state multiplicity of DM annihilation in the current Universe. As was mentioned, since $m_H^{T=0} \neq m_H^{T=T_f}$ for the DM of $M_\chi \simeq 4.85 \text{ TeV}$, no explosion happens in the DM annihilation at the present day. On the other hand, if $m_h^{T=0} = m_h^{T=T_f}$, the high-multiplicity final state channel would be leading in the DM annihilation either at present or the freeze-out epoch. It is important to emphasize here that the DM annihilation receives quantum statistical effects (e.g., stimulated emission) in the early Universe but not in the current Universe. It might lead to a significant discrepancy between these reaction rates. The relic density and indirect signals of scalar-portal DM scenarios should be carefully improved by taking into account the high-multiplicity final state with statistical corrections. These issues will also be investigated in future work.

Summary—Cosmological consequences of the Higgspllosion effect revise our picture of DM. In this *Letter*, we revisit the relic abundance of Higgs-portal DM considering the high multiplicity final state due to the Higgspllosion. A key ingredient for the evolution of DM density is the window function (see Eq. 14), which is obtained by carrying out the thermal average of DM annihilation cross section, considering contributions from both the Higgspllosion and the Higgsperion effects. The Higgspllosion stands for the factorial growth of final-state multiplicity in the transition $h^* \rightarrow nh$, which maintains DM longer in the thermal bath of the SM fields. This high multiplicity transition also makes a major correc-

tion to the regulator of the energetic intermediate Higgs, which retains the unitarity in this transition, referred to as the Higgsperion. The window depends only on the Higgs self-coupling; the peak position is $\sqrt{s} \sim 195m_h$ with a finite width of $\Delta\sqrt{s} \sim \pm 1m_h$ for $\lambda \simeq 0.129$. In a minimal Higgs-portal DM model with these effects, DM of $M_\chi \simeq 4.85 \text{ TeV}$ successfully accounts for the observed relic abundance when the complex coupling to Higgs $\tilde{y}_\chi \sim 1.30i$, without conflicting with either of the direct or indirect constraints. Our result is applicable to a wider class of models with other scalar fields, opening a new window for heavy DM.

Acknowledgments—The authors thank T. Nomura for the helpful discussion. This work is supported in part by the Scientific Research (22K14035 [NH], 22K03638, 22K03602 [MY], 20H05852 [NH,KM,KY]). The works of NH and SE are also supported in part by the MEXT Leading Initiative for Excellent Young Researchers Grant Number 2023L0013. KM is supported by NSF Grants Nos. AST-2108466, AST-2108467, and AST-2308021. This work was partly supported by MEXT Joint Usage/Research Center on Mathematics and Theoretical Physics JPMXP0619217849 [MY].

SUPPLEMENTAL MATERIAL

Explosive production of Higgs particles and implications for heavy dark matter: calculation of the thermally-averaged cross-section

In this *Supplemental Material*, we discuss the details of the cross section through the Higgsploding process and its thermally-averaged quantity. We begin with the formula of the cross section given as Eq. (6) in the main text:

$$\begin{aligned} \sigma &= \sum_n \sigma_{\chi\chi \rightarrow nh} \\ &= \frac{1}{\sqrt{s(s-4|M_\chi|^2)}} \cdot \frac{|\tilde{y}_\chi|^2}{4} \left(1 - \frac{4|M_\chi|^2 \cos^2 \theta_{\tilde{y}}}{s} \right) W(\mathbf{3}) \end{aligned} \quad (12)$$

where the window function $0 \leq W(s) \leq 1$ is given by

$$W(s) = \frac{2sm_h^2 \mathcal{R}(s)}{s^2 + m_h^4 \mathcal{R}(s)^2} = \frac{1}{\cosh[\ln(\mathcal{R}(s)m_h^2/s)]} \quad (14)$$

with the dimensionless reaction rate

$$\mathcal{R}(s) = \sum_n \theta(\sqrt{s} - nm_h) \mathcal{R}_n(s), \quad (15)$$

$$\begin{aligned} \mathcal{R}_n(s) &= \frac{1}{2m_h^2} \frac{1}{n!} \int \frac{d^3 p_{h_1}}{(2\pi)^3} \cdots \frac{d^3 p_{h_n}}{(2\pi)^3} \frac{1}{2E_{h_1} \cdots 2E_{h_n}} (2\pi)^4 \delta^4(p_h - p_{h_1} - \cdots p_{h_n}) |\mathcal{M}(h \rightarrow nh)|^2 \\ &\sim \exp \left[n \left(\frac{2}{\sqrt{3}} \frac{\Gamma(5/4)}{\Gamma(3/4)} \sqrt{\lambda n} + \ln \frac{\lambda n}{4e} + \frac{3}{2} \ln \left(\frac{e}{3\pi} \frac{\sqrt{s} - nm_h}{nm_h} \right) - \frac{25}{12} \frac{\sqrt{s} - nm_h}{nm_h} \right) \right] \end{aligned} \quad (16)$$

introduced in Ref. [21]. Note that the complete picture including the nonperturbative effects is still a subject of ongoing discussions. The dimensionless reaction rate $\mathcal{R}(s)$ increases exponentially at high s as shown in FIG. 4. Applying the above formulae to Eq. (14), we obtain the shape of the window function as seen in FIG. 2 of the main text, which leads to the peak position at $\sqrt{s_{\text{peak}}} = 195.02m_h$. The dependence on the final-state Higgs multiplicity directly reflects the properties of the window function $W(s)$.

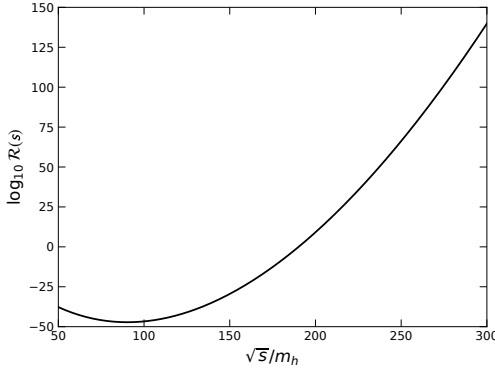


FIG. 4. The plot of the dimensionless reaction rate as a variable \sqrt{s}/m_h .

The thermally-averaged cross section given as Eq. (13) in the main text:

$$\langle \sigma v \rangle = \frac{1}{(n_\chi^{\text{eq}})^2} \cdot \frac{|\tilde{y}_\chi|^2}{32\pi^4} T^4 \int_{4|M_\chi|^2}^\infty \frac{ds}{s} \rho(\sqrt{s}/T) W(s) \quad (17)$$

where ρ is the scattering spectrum, and W stands for the window function. FIG. 5 shows the behavior of $\langle \sigma v \rangle$ varying the number of Higgs bosons produced from the process $\chi\chi \rightarrow nh$ with $n \gg 2$. As seen in FIG. 5, the thermally-averaged cross section continuously grows with $x = M_\chi/T$ for $2m_\chi = 194m_h$ and $198m_h$ while the others show drops at large x , i.e. low T .

Eq. (17) with an approximated estimation of $W(s)$ helps to understand the above behaviors in this context. Expanding the function $\ln(R(s)m_h^2/s)$ around $\sqrt{s} = \sqrt{s_{\text{peak}}}$ with a condition $\mathcal{R}(s_{\text{peak}})m_h^2/s_{\text{peak}} = 1$,

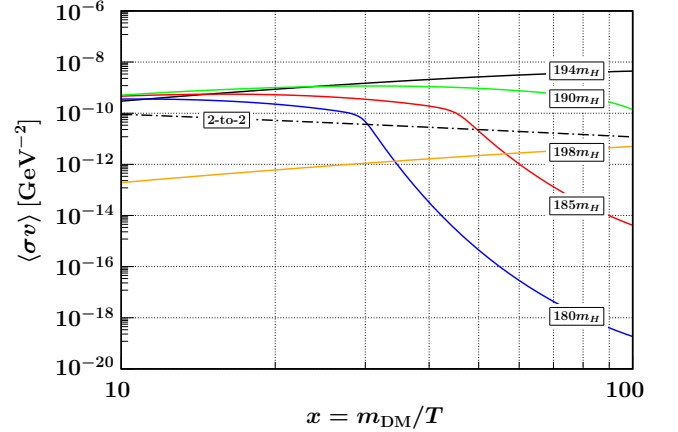


FIG. 5. Evolution of the thermally-averaged cross section for each DM mass. Parameters are set as $\lambda = 0.129$, $m_h = 50$ GeV, and $\tilde{y}_\chi = 1.30i$. The results by the 2-to-2 scattering process is evaluated with $2|M_\chi| = 194m_h = 2 \times 4.85$ TeV.

one obtains

$$\begin{aligned} W(s) &\simeq \frac{1}{\cosh \left[\alpha \frac{\sqrt{s} - \sqrt{s_{\text{peak}}}}{m_h} \right]} \\ &\simeq \frac{1}{2} \exp \left[-\alpha \left(N - N_* + \frac{Ny}{2x} \right) \right], \end{aligned} \quad (18)$$

where $\alpha \equiv \left(\frac{m_h}{\mathcal{R}} \frac{d\mathcal{R}}{ds} - \frac{2m_h}{\sqrt{s}} \right) \Big|_{s=s_{\text{peak}}} \simeq 2.14$. It is useful to scale out with the redefinitions of a constant of $N = 2M_\chi/m_h$ and an integral variable y by $\sqrt{s} = 2M_\chi + Ty$ to obtain the approximated formula of the second line of Eq. 18. N_* corresponds to N at s_{peak} , i.e. $N_* = \sqrt{s_{\text{peak}}}/M_\chi \sim 195$ and we take $\theta_{\tilde{y}} = [\arg M_\chi] = \pi/2$ to maximize the thermally-averaged cross section. Finally, the thermally averaged cross section is obtained as

$$\langle \sigma v \rangle \propto \int_0^\infty dy \sqrt{y} e^{-y} \exp \left[-\alpha \left(N - N_* + \frac{Ny}{2x} \right) \right]. \quad (19)$$

Two sources of the exponential suppression appear in Eq. 19: the first one with e^{-y} originates from the Boltzmann suppression, which effectively restricts the range of y -integral within $0 \leq y \lesssim 1$. The latter is the suppression unique to this model which incorporates the Higgspllosion mechanism. For $N \sim 200 \gtrsim N_*$, the factor $\exp[-\alpha Ny/2x]$ dominates over $\exp[-y]$ up to $x \lesssim$

$\frac{1}{2}\alpha N \sim 214$, and hence this integrant grows in the regime $10 \leq x \leq 10^2$ which we show in the figure. For much larger values of $x \gg 214$, the term with $\exp[-\alpha N y/2x]$ goes to the unity then the thermally-averaged cross section drops by the factor $e^{-\alpha(N-N_*)}$. On the other hand, the damping feature at the lower multiplicity $N \lesssim N_*$ has a different reason. In the early stage of $x \lesssim \mathcal{O}(10)$, the “effective” integration range $0 \leq y \lesssim 1$ covers the peak position of the window enough, while the effective range cannot reach the peak of the window at the later stage $x \gtrsim \mathcal{O}(10)$. This means that the kinetic energy of the annihilating DM particles is insufficient to induce the Higgspllosion.

-
- [1] Gianfranco Bertone, Dan Hooper, and Joseph Silk. Particle dark matter: Evidence, candidates and constraints. *Phys. Rept.*, 405:279–390, 2005. doi:10.1016/j.physrep.2004.08.031.
- [2] Jonathan L. Feng. Dark Matter Candidates from Particle Physics and Methods of Detection. *Ann. Rev. Astron. Astrophys.*, 48:495–545, 2010. doi:10.1146/annurev-astro-082708-101659.
- [3] Vanda Silveira and A. Zee. SCALAR PHANTOMS. *Phys. Lett. B*, 161:136–140, 1985. doi:10.1016/0370-2693(85)90624-0.
- [4] John McDonald. Gauge singlet scalars as cold dark matter. *Phys. Rev. D*, 50:3637–3649, 1994. doi:10.1103/PhysRevD.50.3637.
- [5] C. P. Burgess, Maxim Pospelov, and Tonnies ter Veldhuis. The Minimal model of nonbaryonic dark matter: A Singlet scalar. *Nucl. Phys. B*, 619:709–728, 2001. doi:10.1016/S0550-3213(01)00513-2.
- [6] Hooman Davoudiasl, Ryuichiro Kitano, Tianjun Li, and Hitoshi Murayama. The New minimal standard model. *Phys. Lett. B*, 609:117–123, 2005. doi:10.1016/j.physletb.2005.01.026.
- [7] Brian Patt and Frank Wilczek. Higgs-field portal into hidden sectors. 5 2006.
- [8] Sarah Andreas, Thomas Hambye, and Michel H. G. Tytgat. WIMP dark matter, Higgs exchange and DAMA. *JCAP*, 10:034, 2008. doi:10.1088/1475-7516/2008/10/034.
- [9] Sarah Andreas, Chiara Arina, Thomas Hambye, Fu-Sin Ling, and Michel H. G. Tytgat. A light scalar WIMP through the Higgs portal and CoGeNT. *Phys. Rev. D*, 82:043522, 2010. doi:10.1103/PhysRevD.82.043522.
- [10] Christoph Englert, Tilman Plehn, Dirk Zerwas, and Peter M. Zerwas. Exploring the Higgs portal. *Phys. Lett. B*, 703:298–305, 2011. doi:10.1016/j.physletb.2011.08.002.
- [11] Oleg Lebedev, Hyun Min Lee, and Yann Mambrini. Vector Higgs-portal dark matter and the invisible Higgs. *Phys. Lett. B*, 707:570–576, 2012. doi:10.1016/j.physletb.2012.01.029.
- [12] Xiaoyong Chu, Thomas Hambye, and Michel H. G. Tytgat. The Four Basic Ways of Creating Dark Matter Through a Portal. *JCAP*, 05:034, 2012. doi:10.1088/1475-7516/2012/05/034.
- [13] Shinya Kanemura, Shigeki Matsumoto, Takehiro Nabeshima, and Nobuchika Okada. Can WIMP Dark Matter overcome the Nightmare Scenario? *Phys. Rev. D*, 82:055026, 2010. doi:10.1103/PhysRevD.82.055026.
- [14] Laura Lopez-Honorez, Thomas Schwetz, and Jure Zupan. Higgs portal, fermionic dark matter, and a Standard Model like Higgs at 125 GeV. *Phys. Lett. B*, 716:179–185, 2012. doi:10.1016/j.physletb.2012.07.017.
- [15] Abdelhak Djouadi, Oleg Lebedev, Yann Mambrini, and Jeremie Quevillon. Implications of LHC searches for Higgs-portal dark matter. *Phys. Lett. B*, 709:65–69, 2012. doi:10.1016/j.physletb.2012.01.062.
- [16] Seungwon Baek, P. Ko, Wan-Il Park, and Eibun Senaha. Higgs Portal Vector Dark Matter : Revisited. *JHEP*, 05:036, 2013. doi:10.1007/JHEP05(2013)036.
- [17] Abdelhak Djouadi, Adam Falkowski, Yann Mambrini, and Jeremie Quevillon. Direct Detection of Higgs-Portal Dark Matter at the LHC. *Eur. Phys. J. C*, 73(6):2455, 2013. doi:10.1140/epjc/s10052-013-2455-1.
- [18] Admir Greljo, J. Julio, Jernej F. Kamenik, Christopher Smith, and Jure Zupan. Constraining Higgs mediated dark matter interactions. *JHEP*, 11:190, 2013. doi:10.1007/JHEP11(2013)190.
- [19] Matthew R. Buckley, David Feld, and Dorival Goncalves. Scalar Simplified Models for Dark Matter. *Phys. Rev. D*, 91:015017, 2015. doi:10.1103/PhysRevD.91.015017.
- [20] Giorgio Arcadi, Abdelhak Djouadi, and Marumi Kado. The Higgs-portal for dark matter: effective field theories versus concrete realizations. *Eur. Phys. J. C*, 81(7):653, 2021. doi:10.1140/epjc/s10052-021-09411-2.
- [21] Valentin V. Khoze and Michael Spannowsky. Higgspllosion: Solving the hierarchy problem via rapid decays of heavy states into multiple Higgs bosons. *Nucl. Phys. B*, 926:95–111, 2018. doi:10.1016/j.nuclphysb.2017.11.002.
- [22] Valentin V. Khoze. Multiparticle production in the large λn limit: realising Higgspllosion in a scalar QFT. *JHEP*, 06:148, 2017. doi:10.1007/JHEP06(2017)148.
- [23] Valentin V. Khoze and Sebastian Schenk. Multiparticle amplitudes in a scalar EFT. *JHEP*, 05:134, 2022. doi:10.1007/JHEP05(2022)134.
- [24] Joerg Jaeckel and Sebastian Schenk. Exploring high multiplicity amplitudes: The quantum mechanics analogue of the spontaneously broken case. *Phys. Rev. D*, 99(5):056010, 2019. doi:10.1103/PhysRevD.99.056010.
- [25] Valentin V. Khoze and Joey Reiness. Review of the semiclassical formalism for multiparticle production at high energies. *Phys. Rept.*, 822:1–52, 2019. doi:10.1016/j.physrep.2019.06.004.
- [26] Celine Degrande, Valentin V. Khoze, and Olivier Matelaer. Multi-Higgs production in gluon fusion at 100 TeV. *Phys. Rev. D*, 94:085031, 2016. doi:10.1103/PhysRevD.94.085031.
- [27] James S. Gainer. Measuring the Higgspllosion Yield: Counting Large Higgs Multiplicities at Colliders. 5 2017.
- [28] Valentin V. Khoze, Joey Reiness, Michael Spannowsky, and Philip Waite. Precision measurements for the Higgsploding Standard Model. *J. Phys. G*, 46(6):065004, 2019. doi:10.1088/1361-6471/ab1a70.
- [29] M. V. Libanov, V. A. Rubakov, D. T. Son, and Sergey V. Troitsky. Exponentiation of multiparticle amplitudes in scalar theories. *Phys. Rev. D*, 50:7553–7569, 1994. doi:10.1103/PhysRevD.50.7553.
- [30] M. V. Libanov, D. T. Son, and Sergey V. Troitsky. Exponentiation of multiparticle amplitudes in scalar theories. 2. Universality of the exponent. *Phys. Rev. D*, 52:3679–3687, 1995. doi:10.1103/PhysRevD.52.3679.

- [31] D. T. Son. Semiclassical approach for multiparticle production in scalar theories. *Nucl. Phys. B*, 477:378–406, 1996. doi:10.1016/0550-3213(96)00386-0.
- [32] Yu. Makeenko. Exact multiparticle amplitudes at threshold in large N component ϕ^4 theory. *Phys. Rev. D*, 50:4137–4144, 1994. doi:10.1103/PhysRevD.50.4137.
- [33] Note1. Although both the nonperturbative aspects and the effect of electroweak symmetry restoration for the multiparticle processes are still under debate [41–49], we adopt the expression obtained by Ref. [21, 22, 26] that the explosive production of $\mathcal{O}(100)$ Higgs bosons leads to the factorial growth of scattering amplitude.
- [34] Note2. The summation over all possible n' would result in non-trivial outcomes. A careful investigation incorporating the non-perturbative effects which are originated from t -/ u -channel type processes is required.
- [35] N. Aghanim et al. Planck 2018 results. I. Overview and the cosmological legacy of Planck. *Astron. Astrophys.*, 641:A1, 2020. doi:10.1051/0004-6361/201833880.
- [36] Francesca Calore, Marco Cirelli, Laurent Derome, Yoann Genolini, David Maurin, Pierre Salati, and Pasquale Dario Serpico. AMS-02 antiprotons and dark matter: Trimmed hints and robust bounds. *SciPost Phys.*, 12(5):163, 2022. doi:10.21468/SciPostPhys.12.5.163.
- [37] Andrea Addazi et al. The Large High Altitude Air Shower Observatory (LHAASO) Science Book (2021 Edition). *Chin. Phys. C*, 46:035001–035007, 2022.
- [38] A. Albert et al. Science Case for a Wide Field-of-View Very-High-Energy Gamma-Ray Observatory in the Southern Hemisphere. 2 2019.
- [39] Aria Basirnia, Sebastian Macaluso, and David Shih. Dark Matter and the Higgs in Natural SUSY. *JHEP*, 03:073, 2017. doi:10.1007/JHEP03(2017)073.
- [40] Jessica Goodman, Masahiro Ibe, Arvind Rajaraman, William Shepherd, Tim M. P. Tait, and Hai-Bo Yu. Constraints on Light Majorana dark Matter from Colliders. *Phys. Lett. B*, 695:185–188, 2011. doi:10.1016/j.physletb.2010.11.009.
- [41] M. B. Voloshin. Loops with heavy particles in production amplitudes for multiple Higgs bosons. *Phys. Rev. D*, 95(11):113003, 2017. doi:10.1103/PhysRevD.95.113003.
- [42] S. V. Demidov, B. R. Farkhtdinov, and D. G. Levkov. Suppression exponent for multiparticle production in $\lambda\phi^4$ theory. *JHEP*, 02:205, 2023. doi:10.1007/JHEP02(2023)205.
- [43] A. Curko and G. Cynolter. Unitarity in Multi-Higgs Production. 11 2019.
- [44] Sebastian Schenk. The breakdown of resummed perturbation theory at high energies. *JHEP*, 03:100, 2022. doi:10.1007/JHEP03(2022)100.
- [45] Faye M. Abu-Ajamieh. A Phenomenological Approach to Multi-Higgs Production at High Energy. *Asian Journal of Research and Reviews in Physics*, 6(1):39–56, 2022. doi:10.9734/ajr2p/2022/v6i130177.
- [46] A. Monin. Inconsistencies of higgsplosion. 8 2018.
- [47] Alexander Belyaev, Fedor Bezrukov, Chris Shepherd, and Douglas Ross. Problems with Higgsplosion. *Phys. Rev. D*, 98(11):113001, 2018. doi:10.1103/PhysRevD.98.113001.
- [48] S. V. Demidov and B. R. Farkhtdinov. Numerical study of multiparticle scattering in $\lambda\phi^4$ theory. *JHEP*, 11:068, 2018. doi:10.1007/JHEP11(2018)068.
- [49] S. V. Demidov, B. R. Farkhtdinov, and D. G. Levkov. Numerical Study of Multiparticle Production in ϕ^4 Theory: Comparison with Analytical Results. *JETP Lett.*, 114(11):649–652, 2021. doi:10.1134/S0021364021230028.